Springer

KSME

Journal of Mechanical Science and Technology 32 (1) (2018) 345~350
www.springerlink.com/content/1738-494x(Print)/1976-3824(Online)
DOI 10.1007/s12206-017-1234-6

Experimental investigation of kerf characteristics through wire electrochemical spark cutting of alumina epoxy nanocomposite †

Pallvita Yadav*, Vinod Yadava and Audhesh Narayan

Department of Mechanical Engineering, Motilal Nehru National Institute of Technology Allahabad, 211004, India

(Manuscript Received May 14, 2017; Revised August 24, 2017; Accepted September 20, 2017)

Abstract

Alumina epoxy nanocomposite (AENC) is an emerging class of composites with a wide range of functionality and applicability; however, managing AENC using a machine is difficult because of its special mixed characteristics. The presence of extremely hard alumina particles in soft epoxy matrix enhances material properties. The present work investigates the kerf characteristics of a straight cut made in AENC through Wire electrochemical spark cutting (WECSC) process. The kerf characteristics, such as kerf deviation and taper, are used to measure the cut quality. The applied voltage, electrolyte concentration, wire velocity, pulse on-time and pulse off-time are varied, and their effects on the kerf characteristics are experimentally investigated in a developed setup. Influencing parameters for straight cutting of AENC are applied voltage, concentration of electrolyte and wire velocity.

Keywords: Alumina epoxy nanocomposite; Kerf deviation; Kerf taper; Wire electrochemical spark cutting

1. Introduction

Polymer nanocomposites are composed of a polymer matrix reinforced with different forms of nanofibers or nanopowders made of carbides, oxides, or nitrides. Machining of polymer nanocomposites are difficult due to extremely hard reinforcing material in the soft polymer matrix. Researchers have reported improvements in polymer properties with the nanosize reinforcements. Mohanty et al. [1] studied the improved properties of epoxy by adding nanosize reinforcements. Alumina epoxy nanocomposite (AENC) has well-dispersed nanosize alumina particles as reinforcing agents to enhance the engineering properties of the epoxy matrix. Researchers are constantly seeking efficient machining processes to manage AENCs, which are extremely difficult to machine using conventional techniques due to heavy tool wear because the presence of extremely hard alumina particles.

Wire electrochemical spark cutting (WECSC) has been used to cut electrically non-conductive materials, such as ceramics, glasses, and composites. In 1985, Tsuchiya et al. [2] first used Traveling-wire Electrochemical spark machining (TW-ECSM) process to cut glasses and ceramics. Jain et al. experimentally studied the machining characteristics of Kevlar and glass epoxy composites through the TW-ECSM process [3]. They reported that Material removal rate (MRR) increases with an increase in applied voltage and also analysed the presence of numerous thermal cracks and a wide range of HAZ. Singh et al. [4] examined the effect of applied voltage, workpiece feed rate, and concentration of electrolyte on performance parameters, such as the width of cut and MRR, due to machining of fine slots in borosilicate glass through Wire electrochemical discharge machining (WECDM) process. They analyzed the effect of process parameters on wire breakage problem during machining. Manna and Kundal [5] studied the variation of Material removal (MR) due to varied electrolyte concentration, supply voltage, inter-electrode gap, and wire velocity in the TW-ECSM of alumina. Peng and Liao [6] performed experiments, such as slicing of optical glass and quartz material, through the TW-ECSM process and reported that the pulsed DC provides an improved spark stability. Kuo et al. [7] examined the surface quality of machined quartz glass workpiece through the WECDM process after adding SiC particles in the electrolyte solution. They found that adding SiC particles provides improved surface quality and machining precision.

Bhuyan and Yadava [8] investigated the machining characteristics in terms of MRR and kerf width given that cutting borosilicate glass materials through the TW-ECSM process varies in voltage, electrolyte conductivity, and wire velocity. These researchers observed the variation in MRR and kerf width with an increase in voltage and analyzed the variation of electrolyte concentration during the process. Singh et al. [9] examined the variation of MRR by machining partially electrically conductive PZT ceramic and carbon fiber epoxy com-

*Corresponding author. Tel.: +91 532 2545404, 2545407, Fax.: +91 532 2545341
E-mail address: pallvita@gmail.com
† Recommended by Editor Haedo Jeong

posite through the TW-ECSM process with an increase in electrolyte concentration and voltage. They reported non-uniformity in slot edges due to undesirable sparking. Mitra et al. [10] studied the effect of operating parameters, such as pulse on-time, pulse frequency, applied voltage, wire velocity, and electrolyte concentration on MRR and Radial overcut (ROC) using a groove cut made in Hylam-based composite through the TW-ECSM process. Yang et al. [11] examined the effect of KOH and NaOH electrolyte on slit expansion, roughness, and MRR by machining Pyrex glass through the WECDM process. They reported that adding SiC to the electrolyte solution improves the overcut quality. Bebroozfar and Razfar [12] analyzed the diameter of plasma channel by machining glass during the ECDM process.

Most research works from the relevant literature related to the TW-ECSM process have focused on the machining behavior of non-conducting materials, such as ceramics, glasses and fiber-reinforced composites. This paper aims to investigate the effect of various input parameters on kerf characteristics, such as kerf deviation (K_d) and kerf taper (K_t), for straight cutting of AENC through the WECSC process.

2. Materials and methods

This section describes the setup description and operation, specimen description and fabrication, and experimental procedure for straight cutting of AENC workpiece through the WECSC process.

2.1 Setup description and operation

Fig. 1 illustrates the schematic of the developed WECSC setup used for experiments. The WECSC setup comprises a power supply, machining chamber, automatic workpiece feeding, and wire-traveling units. The positive terminal of pulsating DC power source is connected to an auxiliary electrode (Graphite), and the negative terminal is connected with the active electrode (Wire). The applied voltage varies up to 100 V, and current is up to 3 A. The pulse-on and pulse-off time vary from 1-9999 μs. The machining chamber unit consists a rectangular chamber of plexiglass material with dimensions of 400 mm × 250 mm × 110 mm. The rectangular chamber is used to contain the electrolyte solution for the experiment. The acrylic and metal frames are attached to the machining chamber. Numerous Teflon and metal pulleys are attached to the acrylic frame to guide the wire movement. A controller with a display panel is used to operate the stepper motor through which wires can be attached appropriately, thereby allowing the acquisition of a suitable range of wire velocity. The workpiece holding and feeding arrangement are attached to the metal frame. An auxiliary electrode is placed in a rectangular chamber to maintain the proper inter-electrode gap. The automatic workpiece feeding unit provides a constant feed rate to the workpiece specimen used in the cutting process. The minimum feed motion can be achieved with

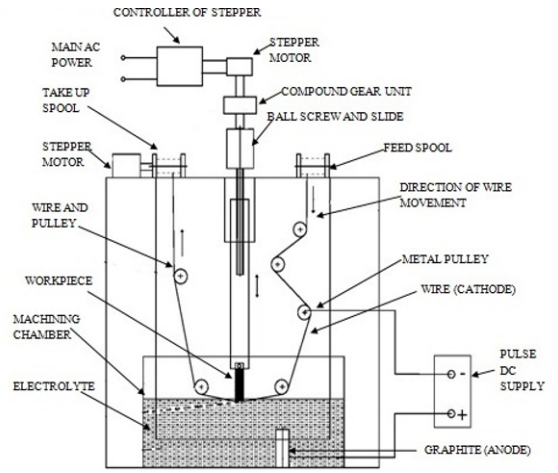

Fig. 1. Schematic of WECSC.

compound gear arrangement ranging from 0.001 mm/sec to 0.01 mm/sec. A brass wire was used as a cathode, whereas a graphite rod (Auxiliary electrode) was used as an anode.

2.2 Specimen description and fabrication

The rectangular cross-section workpiece specimen with dimensions of 30 mm × 25 mm × 3 mm made of AENC was used for experimentation. Initially, the AENC sheet of 3 mm thickness was fabricated using the particulate dispersion technique along with molding. The mold of acrylic material was used to cast the composite. Araldite epoxy was selected as a matrix for the composite material. Alumina nanoparticles with 50 nm average size were considered reinforcing agents. These nanoparticles of 4 wt.% were added to the epoxy resin. The mixture was stirred using a magnetic stirrer at 700 rpm at 65 °C for 2 h. Hardener was added to the mixture after magnetic stirring operation, followed by continuous stirring. The ratio of epoxy resin to hardener was 10:1. The mixture was degassed to remove entrapped air bubbles during the procedure. The mixture was cured by pouring into acrylic molds and maintaining at room temperature for 24 h.

2.3 Experimental procedure

Many exhaustive experiments were performed to decide the input parameter range. A certain number of experiments were performed on the basis of one parameter-at-a-time approach to investigate the input parameter effect. A rectangular cross-section specimen of AENC with dimensions of 30 mm × 25 mm × 3 mm was considered the workpiece sample during the experiment. A brass wire with 0.2 mm diameter was used as a cathode, whereas a graphite rod of 8 mm diameter and 70 mm length was used as an anode. The brass wire was kept in constant contact with the workpiece sample during the straight-cutting process. The inter-electrode gap was set at 60 mm (The distance between the anode and dipped wire at machining zone). Aqueous NaOH solution was used as an electrolyte

Table 1. Experimental conditions.

Workpiece material and thickness	Alumina epoxy nanocomposite (3 mm)
Material of tool (Cathode)	Brass wire (0.2 mm)
Auxiliary electrode (Anode)	Graphite rod
Electrolyte type	Sodium hydroxide (NaOH)
Cutting time	7-10 min
Workpiece feed rate	0.01 mm/s

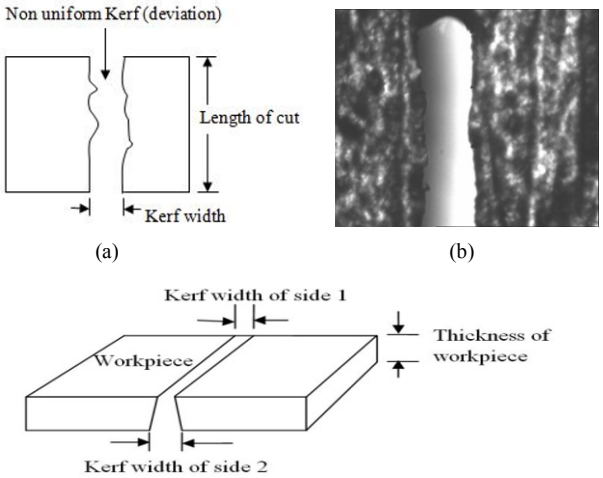

Fig. 2. Schematic of (a) kerf deviation; (b) microscopic image of kerf deviation; (c) kerf taper.

for the experiments. Only a bubble generation (Electrolysis) occurred below 30 V instead of discharge action. The material removal rate was insignificant at low voltage (between 30 and 35 V), and brass wire started to break at above 55 V due to low current carrying capacity of wire; therefore, the range of applied voltage was determined at 40-50 V. The wire was observed to frequently break due to overheating with considerably low wire velocity during the experiments because low wire velocity creates a situation as a stationary tool; however, high wire velocity is inefficient. Therefore, a suitable range of wire velocity was considered for the experiment. For each experiment, the length of the cut was 10 mm. The details of experimental conditions are summarized in Table 1.

Kerf deviation is defined as the difference between the maximum and minimum kerf values. The schematic of kerf deviation and taper is depicted in Figs. 2(a) and (c), respectively, whereas the Kerf deviation measured using an optical microscope (SDM-TR-MSU Sipcon Instrument Industries, India) and the microscopic image are displayed in Fig. 2(b).

Kerf taper (K_t) exists due to varying Kerf widths at the entrance (Side 1) and exit sides (Side 2) of a workpiece specimen and is calculated using Eq. (1).

$$\mathrm{KT(deg)} = \frac{(\text{Kerf width of side 2} - \text{Kerf width of side 1}) \times 180}{2\pi \times \text{workpiece thickness}} \quad (1)$$

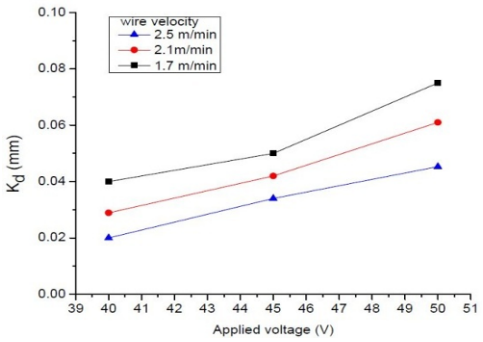

(a)

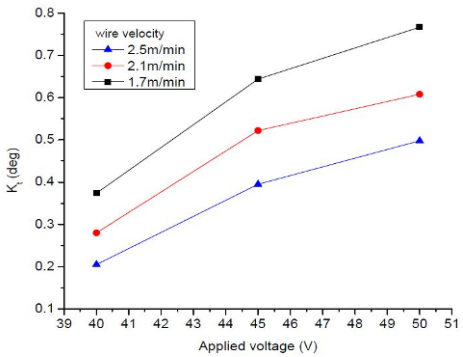

(b)

Fig. 3. Effect of applied voltage on (a) K_d; (b) K_t during straight cutting of AENC workpiece with T_{on} = 350 µs, T_{off} = 300 µs and electrolyte concentration = 250 g/L.

3. Results and discussion

This section describes the effects of various input process parameters on kerf characteristics, such as kerf deviation and taper.

3.1 Effect of applied voltage at different wire velocities

Fig. 3(a) illustrates the variation in kerf deviation for straight cutting of AENC workpiece at different wire velocities to show the effect of the applied voltage.

Kerf deviation increases with varying applied voltage from 40-50 V, as presented in Fig. 3(a). The increase in applied voltage elevates the current density at the tool electrolyte interface (Near the machining zone), which produces numerous hydrogen gas bubbles, and frequently provides a gas film insulation; thus, the rate of spark generation increases the energy per spark. Therefore, an additional amount of material is removed from the workpiece specimen. Kerf deviation decreases when wire velocity increases because an upsurge in wire velocity sweeps the bubbles (The bubbles form an insulating gas film and are responsible for discharge action), thereby resulting in less discharge energy available for material removal; thus, less kerf deviation is obtained. Kerf deviation increases by 50 % when the voltage increased from 45 V to 50 V at 1.7 m/min wire velocity.

Fig. 3(b) indicates the variation of applied voltage on kerf

taper. Kerf is less at the entrance side than the exit side of the workpiece; thus, taper surface exists in the workpiece sample. A new surface of moving wire is exposed continuously at the entrance side of the workpiece therefore less interaction time available between the workpiece and wire; this activity produces less energy for melting of the material. In this paper, the kerf taper increases with varying applied voltage from 40 V to 50 V because more energy is produced at high voltage; this additional energy is abundance for melting the material that increases the taper surface. The nature of curve shows the similar trend at different wire velocities.

3.2 Effect of electrolyte concentration at different wire velocities

The effect of electrolyte concentration on kerf deviation for straight cutting of AENC workpiece is depicted in Fig. 4(a). The kerf deviation increases when the concentration of the solution is increased from 200 g/L to 250 g/L at 1.7 m/min wire velocity and follows a similar trend for different wire velocities. The Kerf deviation reduces by 24 % at 1.7 m/min wire velocity when the concentration is increased from 250 g/L to 300 g/L, because the specific conductance of NaOH used in the experiment is high with the concentration value of approximately 250 g/L, and the specific conductance reduces after this value.

Circuit current increases with an increase in conductivity (or specific conductance) of electrolyte, thereby leading to the acceleration of the electrolysis process and producing numerous hydrogen gas bubbles around the tool electrolyte interface. Thus, spark generation rate increases and producing additional energy that creates a wide cut along the length. This same figure explains the influence of wire velocity on kerf deviation. Moreover, Bhuyan and Yadava [8] reported that the specific conductance of NaOH solution is high at 250 g/L, thereby leading to an increase in conductivity of solution and providing additional energy for melting a material. Paul et al. [13] also explained that the conductivity of electrolyte starts reducing beyond the value of concentration from 25 wt.%, thus providing low current flow and reduced energy.

The kerf deviation decreases while the wire velocity increases because of the less spark interaction time available on the workpiece specimen. Fig. 4(b) demonstrates the variation of electrolyte concentration on kerf taper for straight cutting the AENC workpiece. The kerf taper increases with an upsurge in the concentration of electrolyte from 200 g/L to 250 g/L at 1.7 m/min wire velocity, and kerf taper starts decreasing beyond this value because the specific conductance of used NaOH solution is maximum at 250 g/L and after this value it decreases. Therefore, the conductivity of the electrolyte solution increases and leads to an upsurge in circuit current, followed by increased sparking rate. A large amount of heat generated, which is responsible for further material removal from the workpiece throughout the machining length, results in more kerf taper.

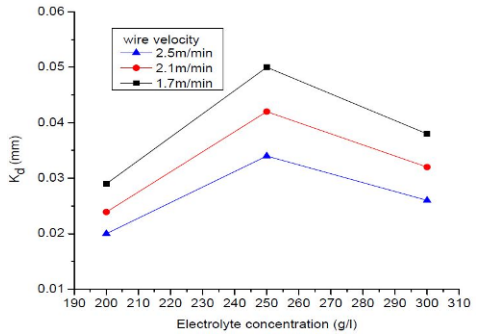

(a)

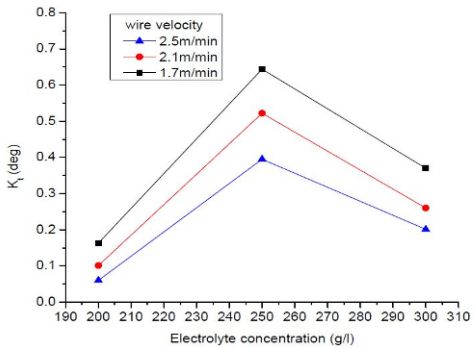

(b)

Fig. 4. Effect of electrolyte concentration on (a) K_d; (b) K_t during straight cutting of AENC workpiece with T_{on} = 350 µs, T_{off} = 300 µs, and applied voltage = 45 V.

Furthermore, the effect of wire velocity is depicted in Fig. 4(b). The interaction time available for spark on workpiece specimen decreases while wire velocity increases; thus, less material is removed from the work sample, thereby resulting in less kerf taper.

3.3 Effect of pulse on-time at different wire velocities

Fig. 5(a) illustrates the variation of kerf deviation with pulse on-time for the different values of wire velocity. Pulse on-time is defined as the time during which machining operation performed. In this work, pulse on-time was considered 300, 350 and 400 µs for the experiment. Kerf deviation increases by 25 % at 1.7 m/min wire velocity while pulse on-time increases from 300-350 µs.

Therefore, the increase in pulse on-time causes an upsurge in spark interaction time on workpiece specimen, or we can say that an increase in heat transfer to the workpiece; thus, a large amount of energy become available to melt the material from the workpiece specimen, thus resulting in high kerf deviation.

The figures for the different wire velocities show a similar trend. Fig. 5(b) indicates that the variation of kerf taper with an increase in pulse on-time for different wire velocities keeping other parameters constant. Kerf taper increases with an upsurge in pulse on-time because the amount of heat transfer

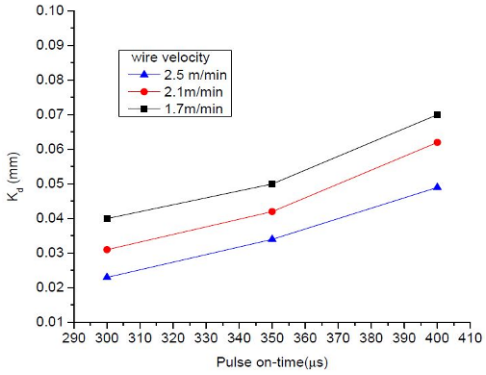

(a)

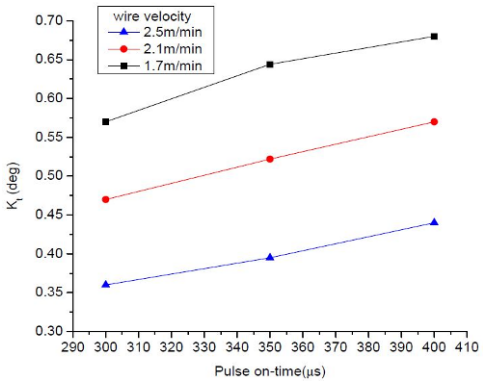

(b)

Fig. 5. Effect of pulse on-time on (a) K_d; (b) K_t during straight cutting of AENC workpiece with electrolyte concentration = 250 g/L, T_{off} = 300 μs, and applied voltage = 45 V.

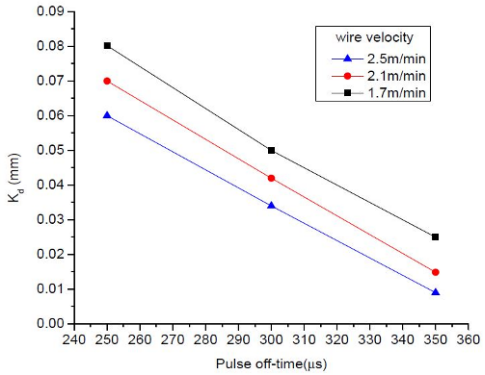

(a)

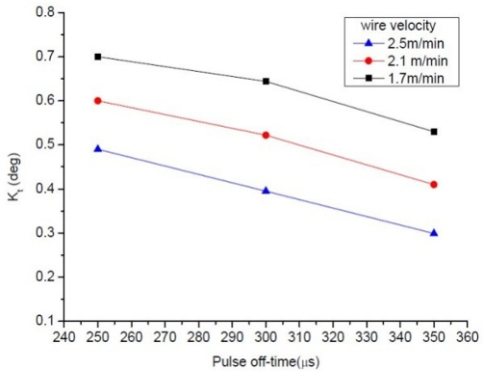

(b)

Fig. 6. Effect of pulse off time on (a) K_d ; (b) K_t during straight cutting of AENC workpiece with electrolyte concentration = 250 g/L , T_{on} = 350 μs, and applied voltage = 45 V.

to workpiece specimen, which is responsible for material removal from workpiece, increases.

3.4 Effect of pulse off-time at different wire velocities

Fig. 6(a) shows the variation in kerf deviation for straight cutting of AENC workpiece at different wire velocities to show the effect of pulse off-time. The effect of pulse off-time at different wire velocities, such as 1.7, 2.1 and 2.5 m/min, are displayed in this figure, thus keeping other parameters constant. The kerf deviation reduces by 37 % at 1.7 m/min wire velocity with an upsurge in pulse off-time from 250 μs to 300 μs. The rate of cooling effect increases between the wire and workpiece sample and less material removed, which results in reduced kerf deviation. The nature of curve shows a similar trend from 300-350 μs.

Fig. 6(b) indicates the variation in kerf taper for straight cutting of AENC workpiece at different wire velocities to show the effect of pulse off-time. Kerf taper reduces when pulse off-time increases because the time span of cooling down the machining zone increases; this activity requires more energy to activate the machining zone. Another reason for this nature of graph may be due to the less interaction of spark on the workpiece, thereby reducing the discharge energy to reduce the amount of material removed from workpiece sample.

4. Conclusions

The following conclusions are drawn after the experimental study on kerf characteristics for straight cutting of AENC through the WECSC process:

(1) The WECSC process for straight cutting of AENC is an effective machining process for nanocomposite materials.

(2) The electrolyte concentration wire velocity and applied voltage are more influencing parameters that affect the cut quality.

(3) Kerf deviation is less at the low applied voltage and high wire velocity.

Acknowledgment

The authors are thankful to Dr. Abhishek Kumar of the Applied Mechanics Department, Motilal Nehru National Institute of Technology Allahabad, India, for the valuable suggestions for specimen preparation. Moreover, the authors acknowledge the Material Development Laboratory, Applied Mechanics Department, Motilal Nehru National Institute of Technology Allahabad, India for the facilities provided in fabricating the AENC specimens.

Nomenclature

K_d : Kerf deviation
K_t : Kerf taper
t_{on} : Pulse on-time
t_{off} : Pulse off-time
V : Applied voltage

References

[1] A. Mohanty, V. K. Srivastava and P. U. Sastry, Investigation of mechanical properties of alumina nanoparticle-loaded hybrid glass/carbon-fiber-reinforced epoxy composites, *Journal of Applied Polymer Science*, 131 (1) (2014) 39749(1-7).

[2] H. Tsuchiya, T. Inoue and M. Miyazaiki, Wire electrochemical discharge machining of glasses and ceramics, *Bulletin Japanese Society of Precision Engineering*, 19 (1) (1985) 73-74.

[3] V. K. Jain, P. S. Rao, S. K. Choudhury and K. P. Rajurkar, Experimental investigations into Traveling wire Electrochemical spark machining (TW-ECSM) of composites, *Transactions of ASME: Journal of Engineering for Industry*, 113 (1) (1991) 75-84.

[4] A. Singh, C. S. Jawalkar, R. Vaishya and A. K. Sharma, A study on wire breakage and parametric efficiency of the wire electro chemical discharge machining process, *Proceedings of the 5th international & 26th AIMTDR Conference,* India (2014) 1-6.

[5] A. Manna and A. Kundal, An experimental investigation on fabricated TW-ECSM setup during micro slicing of nonconductive ceramic, *Int. J. Adv. Manuf. Technol.*, 76 (2015) 29-37.

[6] W. Y Peng and Y. S. Liao, Study of electrochemical discharge machining technology for slicing non-conductive brittle materials, *Journal of Material Processing Technology*, 149 (1-3) (2004) 363-369.

[7] K. Y. Kuo, K. L. Wu, C. K. Yang and B. Yan, Effect of adding SiC powder on surface quality of quartz glass microslit machined by WECDM, *Int. J. Adv. Manuf. Technol.*, 78 (2015) 73-83.

[8] B. K. Bhuyan and V. Yadava, Experimental study of traveling wire electrochemical spark machining of borosilicate glass, *Materials and Manufacturing Processes*, 29 (2014) 298-304.

[9] Y. P. Singh, V. K. Jain, P. Kumar and D. C. Agrawal, Machining piezoelectric (PZT) ceramics using an Electrochemical spark machining (ECSM) process, *Journal of Materials Processing Technology*, 58 (1) (1996) 24-31.

[10] N. S Mitra, B. Doloi and B. Bhattacharyya, Analysis of traveling wire electrochemical discharge machining of Hylam based composites by Taguchi method, *International Journal of Research in Engineering & Technology*, 2 (2) (2014) 223-236.

[11] C. T. Yang, S. L. Song, B. H. Yan and F. Y. Huang, Improving machining performance of wire electro-chemical discharge machining by adding SiC abrasive to electrolyte, *International Journal of Machine Tools and Manufacture*, 46 (15) (2006) 2044-2050.

[12] A. Behroozfar and M. R. Razfar, Experimental and numerical study of material removal in Electrochemical discharge machining (ECDM), *Materials and Manufacturing Processes*, 31 (2016) 495-503.

[13] L. Paul, S. S. Hiremath and J. Ranganayakulu, Experimental investigation and parametric analysis of electro chemical discharge machining, *Int. J. Manufacturing Technology and Management,* 28 (1/2/3) (2014) 57-79.

Pallvita Yadav is currently pursuing Ph.D. in the Department of Mechanical Engineering, Motilal Nehru National Institute of Technology Allahabad, Allahabad (India). Her research area includes advanced machining process.

Vinod Yadava is a Professor and is the Head of the Department of Mechanical Engineering, Motilal Nehru National Institute of Technology Allahabad, Allahabad (India). His research areas include development and performance study/modeling and optimization of advanced multi-scale machining processes, finite element method, and design of experiments in manufacturing.

Audhesh Narayan is an Assistant Professor in the Department of Mechanical Engineering, Motilal Nehru National Institute of Technology Allahabad, Allahabad (India). His research area includes conventional and unconventional manufacturing processes and finite element method in the manufacturing process.